Journal of Theoretical and Applied Physics (JTAP), Special Issue: AICIS'23-Article 17

Proceeding of the 3rd Annual International Conference on Information and Sciences 2023, University of Fallujah, Iraq

https://dx.doi.org/10.57647/j.jtap.2024.si-AICIS23.17

Scherrer and Williamson-Hall estimated particle size using XRD analysis for cast aluminum alloys

Sukaina Iskandar Yusuf*, Sabri Jasim Mohammad, Mohsin Hasan Ali*

Collage of Education for Pure Science, Physics Department, Tikrit University, Iraq.

***Corresponding author:** sokayna.e.yussuf@tu.edu.iq, muhsin.astro@tu.edu.iq

Original Research

Published online: 15 June 2024

Abstract:

Aluminum metal matrix composites find applications in several industries, such as aerospace, military, cars, sports equipment, and electronics. The primary objective of this experimental study is to obtain insights into the microstructural properties of an Al-Zn alloy that has been strengthened with copper. This investigation involved the preparation of an alloy including aluminum and zinc, which was afterward reinforced with varying quantities (0%, 0.4%, 1.2%, and 2%) of copper. In addition to conducting XRD tests to investigate the crystallite structure, particle size, and microscopic strain of the samples using the Scherrer and Williamson-Hall models, structural examinations were carried out using the EDS test to ascertain the elemental composition proportions. It was observed that the alloy (A-Zn-0.4%Cu) has smaller particle sizes than the other alloys under consideration.

Keywords: Aluminum alloys; Crystallite size; Microstructural; Micro-strain; Structural analysis

1. Introduction

Aluminum alloys are formed through the amalgamation of copper, zinc, silicon, lithium, and various other alloy constituents, thereby imparting novel structural, mechanical, and physical characteristics. Due of their notable importance in the realm of aircraft construction, coatings, radiation protection, and electronic systems. This is mostly owing to their advantageous qualities, namely their lightweight nature, high strength, and coefficient of thermal expansion [1].

The lack of perfection observed in crystals can be ascribed to their limited dimensions, as a crystal of infinite size would continue endlessly in all spatial dimensions. The phenomenon of diffraction peak broadening is observed when materials lack full crystallinity. The main objective of peak width analyses is to provide insights into the dimensions of particles and the level of strain inside the lattice structure. The evaluation of lattice strain entails the examination of how crystal imperfections, such as lattice dislocations, affect the distribution of lattice constants. Apart from grain boundaries, many forms of strain unrelated to grain boundaries can be observed, such as sinter stresses, stacking faults, and coherency stresses [2].

The atomic characteristics of a solid substance, particularly in metals, are commonly employed to characterize its qualities. XRD profile analysis is the prevailing methodology used to evaluate the dimensions of crystallites. This method employs an average approach. In addition to the Scherrer method, researchers also utilize alternate approaches, such as the Williamson-Hall (W-H) method to examine the impact of strain on the determination of particle size. We are particularly interested in determining the extent to which strain influences the size of crystallites [3–5].

In this study, the Scherrer and Williamson Hall models were employed to examine the impact of different copper to (Al-Zn) weight ratios on the particle size and microscopic strain of the specimens.

2. Experimental procedure

To initiate the production of the alloys under investigation, pure aluminum was initially measured using a precise electrobalance with a precision of 0.0001. Following that, the respective amounts of the components used in the foundry were computed to attain the desired weight proportions for each specific ingot (as shown in Table 1).

Aluminum was melted at 750 °C in an electric furnace (with a graphite-clay boat). The pure zinc was then added after it

Table 1. Sample composition and weight ratio.

Alloys	Al	Zn	Cu
S1	90.0%	10%	-
S2	89.6%	10%	0.4%
S3	88.8%	10%	1.2%
S4	88.0%	10%	2.0%

was wrapped in pure aluminum foil (to prevent oxidation and burning when it came into touch with the molten) and the molten was continually stirred using an electric mixer with a rotating speed of 200 (rad/min).
By adding aluminum chloride to the melt, the bubbles and gases were removed, and the mixture was thoroughly mixed. The slag is then scraped from the molten metal's surface. To avoid hot cracking, the temperature of the casting mold was raised to 200 °C before pouring the molten metal into it. The molten metal is cooled after it is placed in the casting mold. The samples were subsequently cut into small disc-shaped sections 1 cm thick and 1.2 cm in diameter for structural studies. The rest of the copper-reinforced alloys under Study were made in the same way, with copper added to the base alloy in varied weight percentages (as shown in Table 1).

3. Results and discussion

3.1 XRD data analysis

The samples underwent X-ray diffraction (XRD) analysis utilizing a (Philips PAN-analytical X'Pert of XRD) system. The radiation source was (Cu-Kα) with a range from (10° to 80°), step value of 0.1°, wavelength of 1.5404 $\AA$, and an accelerating voltage of 40 kV. All of the samples were tested at laboratory temperature. The results and data that were gathered were then compared to the international standard cards known as JCPDS (Figs. 1, 2, 3, 4).
Crystalline and amorphous materials can be studied and analyzed using X-ray diffraction (XRD). X-ray wavelength (λ) equals atomic level distance (d) according to Bragg's Law, (as show in Tables 2-5). As demonstrated here, Bragg's law applies to Bragg's reflection peaks from parallel crystal surfaces [6].

$$n\lambda = 2d\sin\theta \tag{1}$$

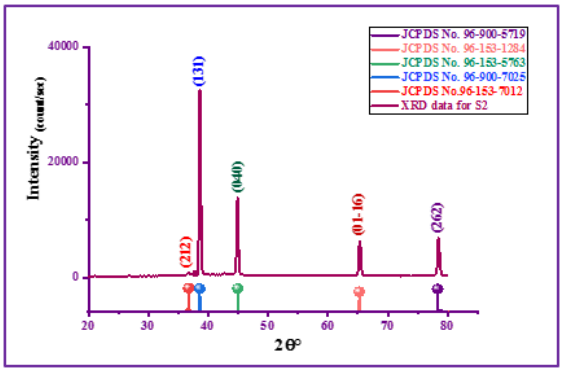

Figure 2. XRD analysis for S2 alloy.

3.2 Scherrer method

Peak broadening is calculated using the Scherrer formula, but it only accounts for crystallite size, not the intrinsic strain that occurs in nano-crystals due to point defects, grain boundaries, triple junctions, and stacking defects [7]. Equation corrects instrumental broadening as shown in Eq. (2) [7–9]:

$$\beta_{hkl}^2 = \beta_{meas.}^2 - \beta_{inst.}^2 \tag{2}$$

where $\beta_{meas.}$ is the measured broadening, $\beta_{inst.}$ is instrumental broadening and β_{hkl} is the corrected broadening. The sample's (FWHM) widened. From β_{hkl} the Scherrer formula Eq. (3) can calculate the average particle size:

$$D = \frac{K\lambda}{\beta_{hkl}\cos\theta} \tag{3}$$

Where K: Scherrer constant = 0.9, λ: X-ray wavelength, θ: peak position, D: the average of particle size.
We derive this result by first taking ln of Eq. (3), and then rearranging it:

$$\ln\beta_{hkl} = \ln\frac{1}{\cos\theta} + \ln\frac{K\lambda}{D} \tag{4}$$

Eq. (4) called the modified Scherrer equation. By comparison Eq. (4) with straight line equation:

$$y = mx + c \tag{5}$$

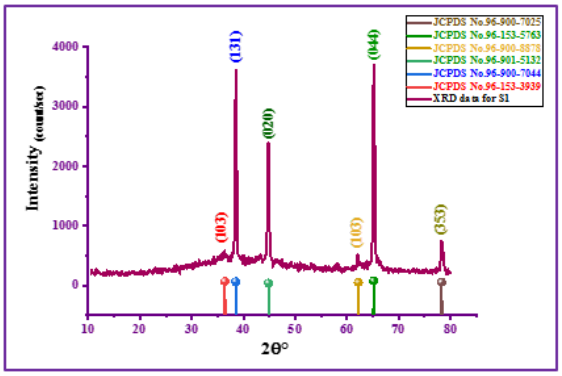

Figure 1. XRD analysis for S1 alloy.

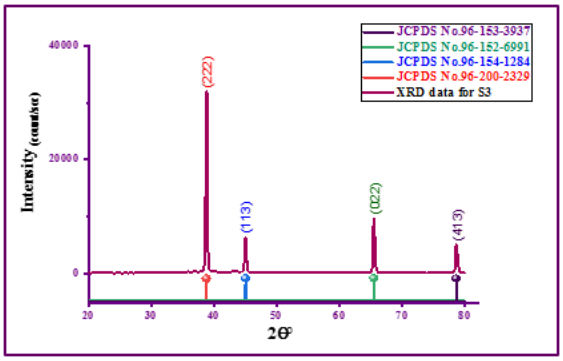

Figure 3. XRD analysis for S3 alloy.

Table 2. XRD test results for S1 alloy.

Chemical formula	Crystallite system	2θ (degree)	$d_{measured}$ (Å)	$d_{standard}$ (Å)	Rel. Intensities%
$Al_{10.64}O_{16}$	Tetragonal/I41/amd/141	37.5390	2.3940	2.37977	16.30
$Zn_8Al_{16}O_{32}$	Cubic/Fd-3m/227	38.4862	2.3391	2.34877	89.65
$Al_{2.66}O_4$	Cubic/Fm-3m/225	44.8168	2.02236	1.97500	68.92
Zn_2O_2	Hexagonal /P63mc/186	62.162	1.49334	1.47735	04.95
$Al_{19.2}O_{32}Zn_{2.4}$	Cubic/Fd-3m/227	65.1275	1.43234	1.41421	100.0
$Zn_8Al_{16}O_{32}$	Cubic/Fd-3m/227	78.3608	1.21928	1.22502	15.59

Table 3. XRD test results for S2 alloy.

Chemical formula	Crystallite system	2θ (degree)	$d_{measured}$ (Å)	$d_{standard}$ (Å)	Rel. Intensities%
$Al_{31.99}O_{48}$	Tetragonal/P-4m2/115	36.7467	2.44581	2.44966	1.48
$Zn_8Al_{16}O_{32}$	Cubic/Fd-3m/227	38.6247	2.33110	2.34033	100
$Al_{19.2}O_{32}Zn_{2.4}$	Cubic/Fd-3m/227	44.9462	2.01684	2.0000	37.27
$Al_{12.6}Zn_{2.1}Cu_{9.6}$	Hexagonal/R3/146	65.2328	1.43028	1.4325	15.96
$Cu_8Al_{16}O_{32}$	Cubic/Fd-3m/227	78.3679	1.21919	1.21826	18.39

Table 4. XRD test results for S3 alloy.

Chemical formula	Crystallite system	2θ (degree)	$d_{measured}$ (Å)	$d_{standard}$ (Å)	Rel. Intensities%
$Cu_8Al_{16}O_{32}$	Cubic/F-43m/216	38.8527	2.31795	2.33536	100
$Al_{12.6}Zn_{2.1}Cu_{9.6}$	Hexagonal/R3/146	45.0523	2.01234	1.99585	19.59
Cu_4O_4	Monoclinic/C12/C1/15	65.4924	1.42524	1.41601	30.27
$Al_{10.64}O_{16}$	Tetragonal/I41/amd/141	78.6431	1.21561	1.21497	15.80

Table 5. XRD test results for S4 alloy.

Chemical formula	Crystallite system	2θ (degree)	$d_{measured}$ (Å)	$d_{standard}$ (Å)	Rel. Intensities%
Cu_4O_4	Monoclinic/C12/C1/15	39.0963	2.30406	2.33946	100
$Al_{12.6}Zn_{2.1}Cu_{9.6}$	Hexagonal/R3/146	45.2533	2.00387	2.04793	64.92
$Cu_8Al_{16}O_{32}$	Cubic/F-43m/216	65.5914	1.42333	1.43048	44.93
$Al_{10.64}O_{16}$	Tetragonal/I41/amd/141	78.8382	1.21309	1.21497	9.01

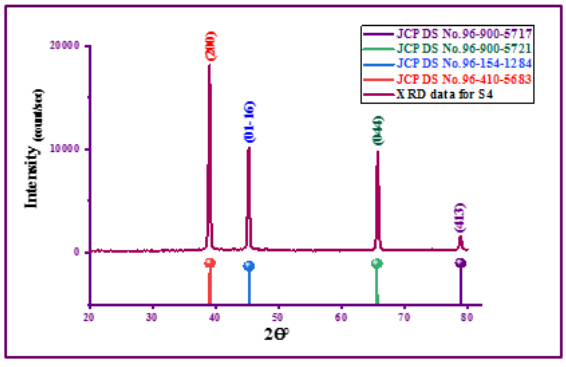

Figure 4. XRD analysis for S4 alloy.

We can make a graph out of $\ln[1/\cos\theta]$ on x-axis and $\ln\beta_{hkl}$ on y-axis (as shown in Figs. 5 and 6). We can calculate the average of the particle size by Intercept $c = \ln[K\lambda/D]$ (as shown in Table 6).

3.3 Williamson-Hall method

The Williamson-Hall technique accounts for the broadening of peaks by considering the dependence of peak width on the 2θ angle. This broadening is attributed to the combined effects of lattice strain and defects. X-ray peaks are consequently influenced by both lattice strain and lattice imperfections. This allows the method to accurately determine peak broadening. Because of this, the overall expansion can

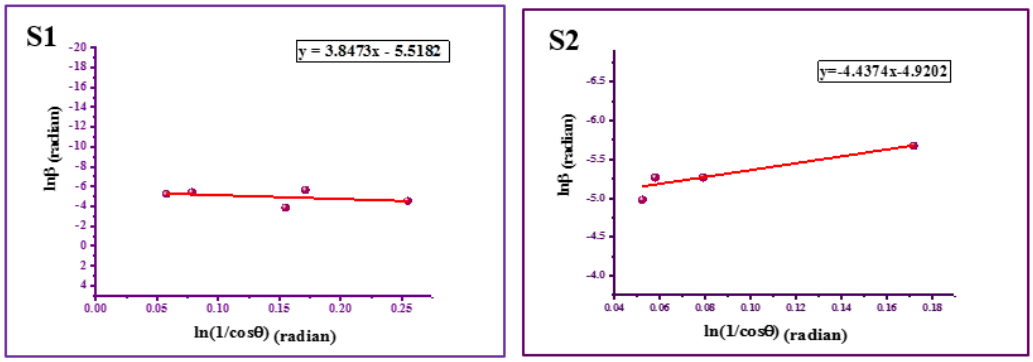

Figure 5. Scherrer method plot for (S1 and S2) alloys.

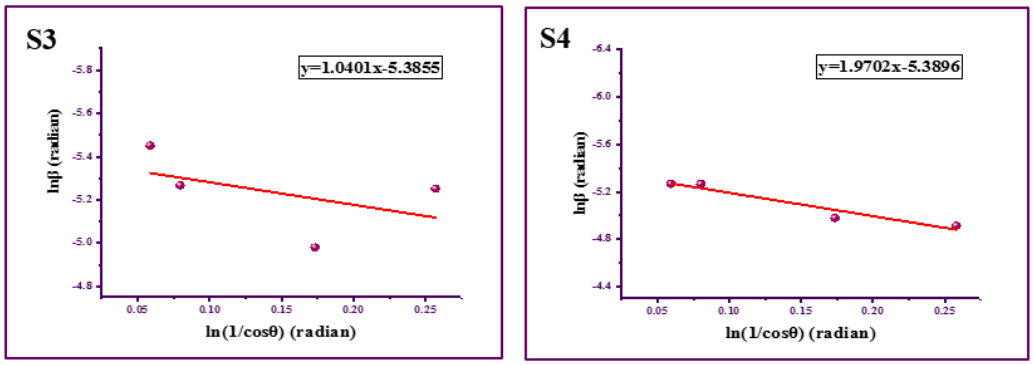

Figure 6. Scherrer method plot for (S3 and S4) alloys.

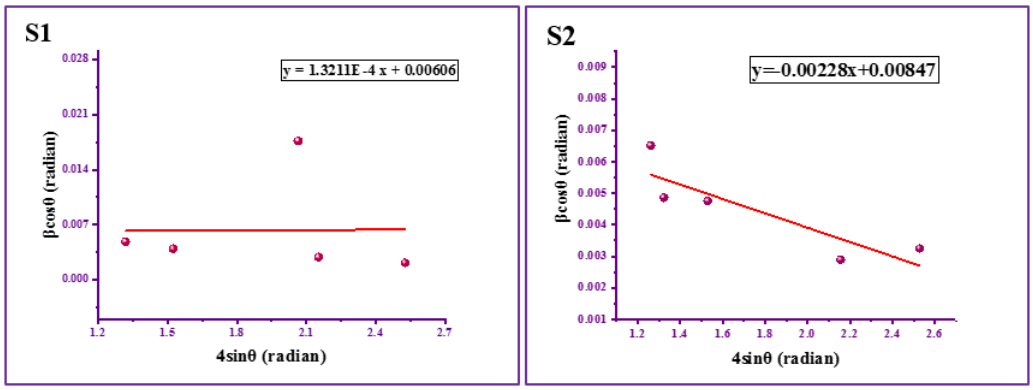

Figure 7. W-H method plot for (S1 and S2) alloys.

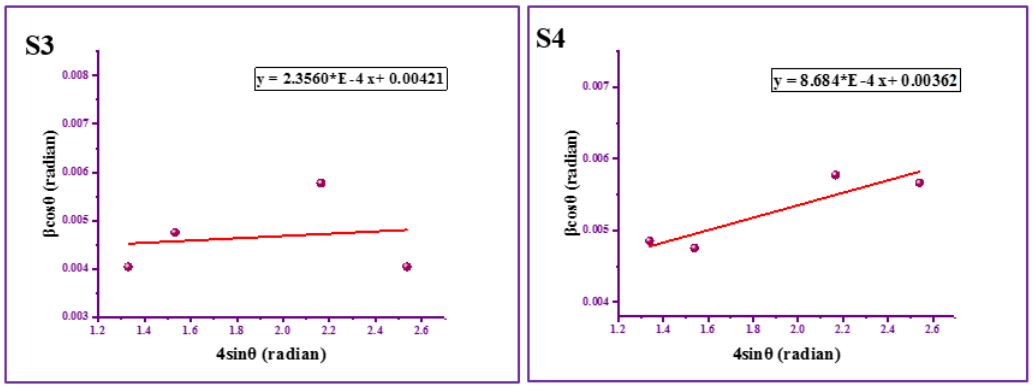

Figure 8. W-H method plot for (S3 and S4) alloys.

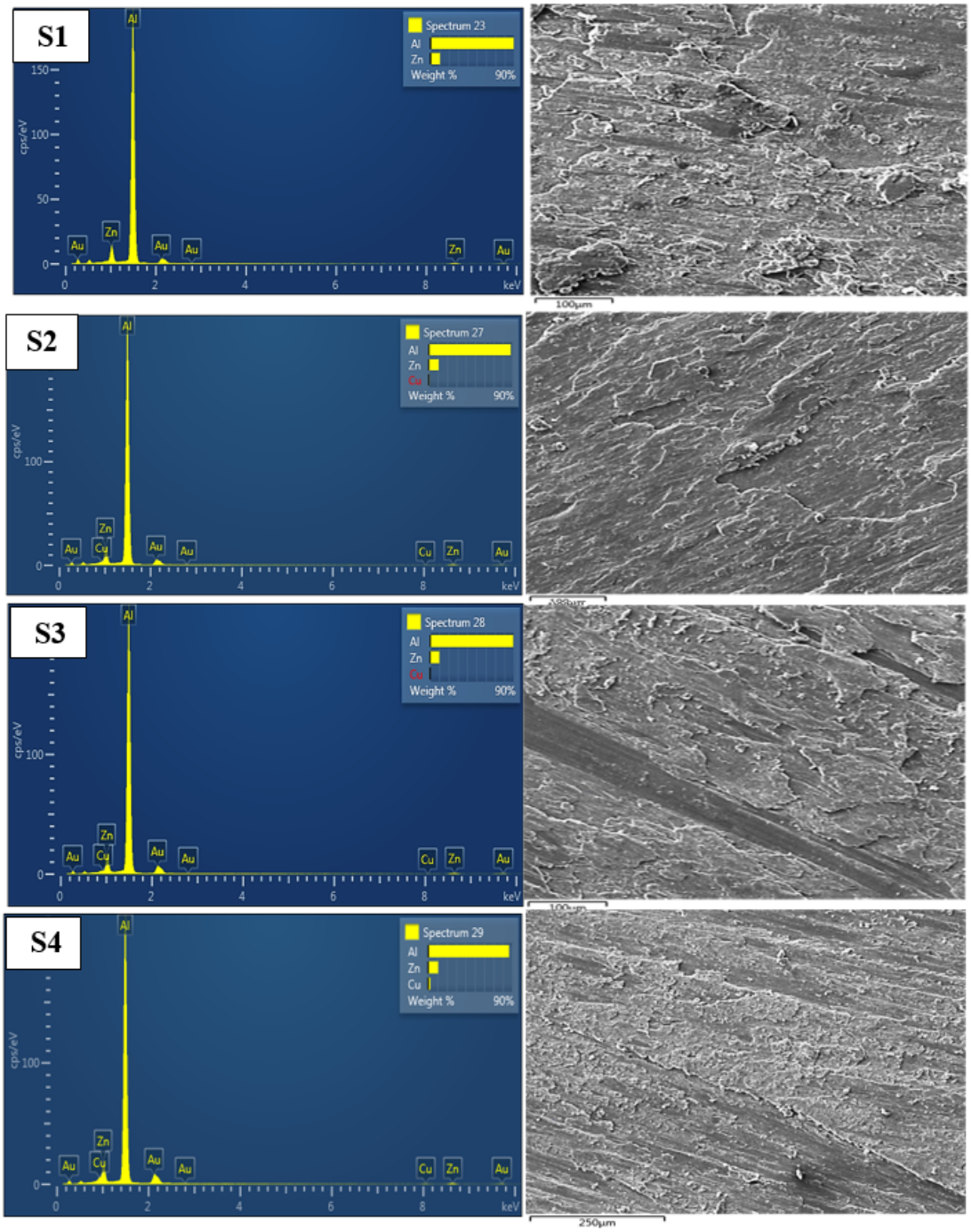

Figure 9. EDS analysis and FE-SEM images for (S1, S2, S3 and S4) alloys.

Table 6. Geometric parameters for (S1, S2,S3 and S4) alloys by Scherrer and Williamson-Hall methods.

Sample	Scherrer	Williamson-Holl	
	D (nm)	D (nm)	Strain
S1	34.5506	22.8802	0.00390
S2	18.9997	16.3700	-0.00228
S3	30.2569	32.9344	2.356E-4
S4	30.3812	38.3022	8.684E-4

be expressed as [3, 10]:

$$\beta_{total} = \beta_{size} + \beta_{strain} \quad (6)$$

where: β_{total} is total broadening., β_{size} is the caused broadening by size and β_{strain} is the broadening by strain.
Utilizing the uniform deformation model (UDM), the average particle size and micro-strain were ascertained, which is a modified version of the W-H equation. This model accounts for the isotropic strain imposed by nano-crystal defects along the crystallographic axis. The strain-induced peak expansion, which is caused by this intrinsic strain, can be expressed as [11, 12]:

$$\beta_{hkl} \cos\theta = \frac{K\lambda}{D} + 4\varepsilon \sin\theta \quad (7)$$

The isotropic nature of crystals is accounted for by the straight-line Eq. (7). (Figs.7 and 8) show the graphing of Eq. (7).
Particle size and strain for (S1, S2, S3, and S4) alloys can be determined from the y-intercept and slope, respectively, (Table (6)). The literature suggests that compressive strain is present when the plot slope is negative, while tensile strain is present when the plot slope is positive [13].
The observed particle sizes in the Al-Zn-0.4%Cu samples are relatively smaller than those in the samples with different Cu concentrations (0% Cu, 1.2% Cu, and 2% Cu). This means saturation of copper in the α phase with an increase in copper concentration of 0.4%, which may be attributed to the mechanism of solidification of the solid solution and the rearrangement of atoms in these alloys. The addition of

Table 7. Elements concentration in S1 alloy.

Element	Line type	Apparent concentration	*k* ratio	Wt%	Wt% Sigma	Atomic %	Standard lable
Al	K-series	24.56	0.17637	89.72	0.18	95.49	Al_2O_3
Zn	L-series	1.92	0.01924	10.28	0.18	4.51	Zn
Total:				100.00		100.00	

Table 8. Elements concentration in S2 alloy.

Element	Line type	Apparent concentration	*k* ratio	Wt%	Wt% Sigma	Atomic %	Standard lable
Al	K-series	29.65	0.21297	88.32	0.29	94.82	Al_2O_3
Cu	L-series	0.19	0.00188	0.80	0.22	0.37	Cu
Zn	L-series	2.49	0.02490	10.87	0.22	4.82	Zn
Total:				100.00		100.00	

Table 9. Elements concentration in S3 alloy.

Element	Line type	Apparent concentration	*k* ratio	Wt%	Wt% Sigma	Atomic %	Standard lable
Al	K-series	27.86	0.20013	89.38	0.29	95.32	Al_2O_3
Cu	L-series	0.06	0.00058	0.27	0.22	0.12	Cu
Zn	L-series	2.20	0.02201	10.35	0.22	4.55	Zn
Total:				100.00		100.00	

Table 10. Elements concentration in S4 alloy.

Element	Line type	Apparent concentration	*k* ratio	Wt%	Wt% Sigma	Atomic %	Standard lable
Al	K-series	27.35	0.19647	86.62	0.31	93.98	Al_2O_3
Cu	L-series	0.56	0.00560	2.51	0.24	1.15	Cu
Zn	L-series	2.30	0.02297	10.87	0.23	4.87	Zn
Total:				100.00		100.00	

copper leads to the appearance of the θ phase, which works to increase the hardness and brittleness of these alloys, and this is consistent with previous studies [14, 15].
According to the literature, a downward slope in the plot suggests the existence of compressive strain, whereas an upward slope suggests the potential presence of tensile strain [12]. The data above indicates that the (Al-Zn-0.4%Cu) sample exhibits a negative slope, indicating the presence of compressive strain. Conversely, the samples with varying Cu concentrations (0% Cu, 1.2% Cu, and 2% Cu) show a positive slope, indicating the existence of tensile strain. Lattice strain mostly arises from the expansion or contraction of the nanocrystals' lattice due to slight modifications in the atomic structure, known as size confinement [8].

3.4 EDS data analytic

EDS analysis was performed using the (FE-SEM system in Iran) to determine the elemental concentrations in the samples under investigation. see (Fig. 9) and (Tables 7, 8, 9, 10).

4. Conclusion

Aluminum alloys are important in aircraft construction, coatings, radiation protection, and electronics. XRD analysis was used to study the crystalline structure of the Al-Zn alloys reinforced with (0%, 0.4%, 1.2%, and 2%) copper, and the particle size was calculated by Scherrer's model and Williamson's Hall model: The Williamson-Hall model provides values for particle size D and crystalline micro-strain ε, whereas the Scherrer model only provides approximation. Both of models exhibit the same behavior of particle size. The particle sizes in Al-Zn-0.4%Cu are smaller than those in the samples (0% Cu, 1.2% Cu, and 2% Cu), respectively. In the (Al-Zn-0.4%Cu) alloy, the micro-strain takes negative values, representing a compressive strain, whereas in the samples (0% Cu, 1.2% Cu, and 2% Cu), respectively, the micro-strain takes positive values, indicating an elongative strain. That is, it stands for a tensile strain in those samples.

Authors Contributions
Authors have contributed equally in preparing and writing the manuscript.

Availability of data and materials
Data presented in the manuscript are available via request.

Conflict of Interests
The author declare that they have no known competing financial interests or personal relationships that could have appeared to influence the work reported in this paper.

References

[1] Y. I. Sukaina, M. M. Mohammed, and A. A. Abdulkader. "Crystal diffraction techniques were used to investigate the structural properties of some aluminum alloys.". *IOP Conf. Series: Earth and Environmental Science*, **961**:1–9, 2022.

[2] J. Zhang, Y. Zhang, K. W. Xu, and V.Ji. "General compliance transformation relation and applications for anisotropic hexagonal metal.". *Solid State Commun.*, **139**:87–91, 2006.

[3] V. Mote, Y. Purushotham, and B. Dole. "Williamson-Hall analysis in estimation of lattice strain in nanometer-sized ZnO particles.". *Journal of Theoretical and Applied Physics*, **6**:1–8, 2012.

[4] N. B. Sapn, K.Vinod, and S. K. Singh. "X-ray analysis of $NiFe_2O_4$ nanoparticles by Williamson-Hall and size-strain plot method.". *Journal of Advanced Physics*, **6**:1–4, 2017.

[5] K. Mehjabeen, M. J. Ashutosh, and P. Sh. Shukla. "X-ray analysis of $BaTiO_3$ ceramics by Williamson-Hall and size strain plot methods.". *Conference Paper in AIP Conference Proceedings*, :020138–1–4, 2019.

[6] E. A. Mohammed. "A comparative study of the method of Williamson Hall and the pattern of cadmium oxide nanoparticles for X-rays.". *Turkish Journal of Computer and Mathematics Education*, **12**:881–889, 2021.

[7] H. Irfan, R. K. Mohamed, and S. Anand. "Microstructural evaluation of $CoAl_2O_4$ nanoparticles by Williamson–Hall and size–strain plot methods.". *Journal of Asian Ceramic Societies*, **6**:1–9, 2018.

[8] K. Pratishtha and C. Pratima. "Microstructural evaluation of iron oxide nanoparticles at different calcination temperature by Scherrer, Williamson-Hall, Size-Strain Plot and Halder-Wagner methods. ". *Phase Transitions A Multinational Journal*, **94**:731–753, 2021.

[9] Y. Sadegh, G. Behrooz, and P. N. Maria. "Morpho/Opto-structural characterizations and XRD-assisted estimation of crystallite size and strain

in MgO nanoparticles by applying Williamson–Hall and size–strain techniques. ". *Journal of Cluster Science*, **33**:2197–2207, 2021.

[10] C. U. Nikam, S. R. Kadam, R. S. Shitole, A. P. Birajdar, V. K. Barote, S. R. Wadgnae, R. H. Kadam, and G. H. Kale. "Williamson-Hall and Size-strain plot based micro-structural analysis and evaluation of elastic properties of Dy3+ substituted Co-Zn nano-spinels.". *Journal of Physics: Conference Series*, **2426**:1–9, 2023.

[11] B. Hariyant, D. A. P. Wardani, N. Kurniawati, N. P. Har, N. Darmawan, and Irzaman. "X-ray peak profile analysis of silica by Williamson–Hall and size-strain plot methods. ". *Journal of Physics: Conference Series*, **2019**:1–5, 2021.

[12] B. Bandna, P. B. Barman, and K. Rajesh. "XRD analysis of undoped and Fe doped TiO_2 nanoparticles by Williamson Hall method. ". *4th National Conference on Advanced Materials and Radiation Physics (AMRP-2015)*, :030025–1–4, 2020.

[13] R. Das and S. Sarkar. "Determination of intrinsic strain in poly(vinylpyrrolidone)-capped silver nano-hexapod using X-ray diffraction technique. ". *Curr Sci.*, **109**:775–778, 2015.

[14] S. Temel, B. Osman, and A. Yasin. "Developing aluminium–zinc-based a new alloy for tribological applications.". *J Mater Sci.*, **44**:1969–1976, 2009.

[15] S. S. Irhayyim, R. A. Saad, and A. A. Abdulkader. "Mechanical performance of micro-Cu and nano-Ag reinforced Al-CNT composite prepared by powder metallurgy technique. ". *Materials Research Express*, **6**:11, 2019.